

PAPER • OPEN ACCESS

Raman spectroscopy of unknown mineral sample by solar pumped laser system

To cite this article: Yasser A Abdel Hadi *et al* 2020 *J. Phys.: Conf. Ser.* **1472** 012006

View the [article online](#) for updates and enhancements.



IOP | ebooks™

Bringing you innovative digital publishing with leading voices to create your essential collection of books in STEM research.

Start exploring the collection - download the first chapter of every title for free.

Raman spectroscopy of unknown mineral sample by solar pumped laser system

Yasser A Abdel Hadi¹, M S Abo Ghazala², Samir A Yousef²,

U Ali Rahoma¹, Ahmed A Elminawy¹

1- National Research Institute of Astronomy and Geophysics (NRIAG), Solar and Space Research Department, Helwan, Cairo, Egypt

2- Menoufia University, Faculty of Science, Physics Department, Egypt

E-mail:Ahmedabdou63@hotmail.com

Abstract: -A detailed Raman spectroscopy study on an unknown sample by using compact solar-pumped (Nd:YAG) laser as an excitation source is simulated by using a primary parabolic concentrator mirror, Compound Parabolic Concentrator (CPC) to be used as an off-grid technique for identification unknown mineral samples. The unknown sample is exposed to the laser beam as the source of exciting photons at wavelength 532 nm. The frequencies of the scattered light are measured by using a highly sensitive spectrometer which detects in the range of (350 - 1150nm) with an optical resolution of 0.2 nm and 600 g/mm. The data are processed by an optical spectroscopy software to be compared with reference libraries. This study shows that the use of solar laser in the field of Raman spectroscopy is advantageous in increasing the precision of analyzing the materials and accordingly in reducing the costs of the analyzing process.

Introduction

Raman spectroscopy is an optical spectroscopic technique that has been used for decades for the spectral identification and detection of a wide range of chemical species. It often uses a high power laser to excite the weak Raman excitation emission lines from material, where the Raman emission is shifted in wavelength by a unique value that can be used to identify the material (1).

Raman spectroscopy has been utilized for many years as a complimentary tool to IR absorption spectroscopy for the investigation of vibrational and rotational spectra of molecules (2). The advantage of Raman spectroscopy as compared to the regular IR absorption spectroscopy is the ability to investigate molecules without an initial dipole moment even though the intensity of Raman emission is comparatively weak. Raman



spectroscopy has become a useful analytical tool ever since the invention of the laser. A typical point Raman spectroscopy setup is presented in Fig. 1. As it can be seen, a typical setup usually includes a cw or pulsed laser to excite the sample molecules, collection optics to collect the Raman scattering signal, a CCD detector and a computer to process the spectrum and control the setup.

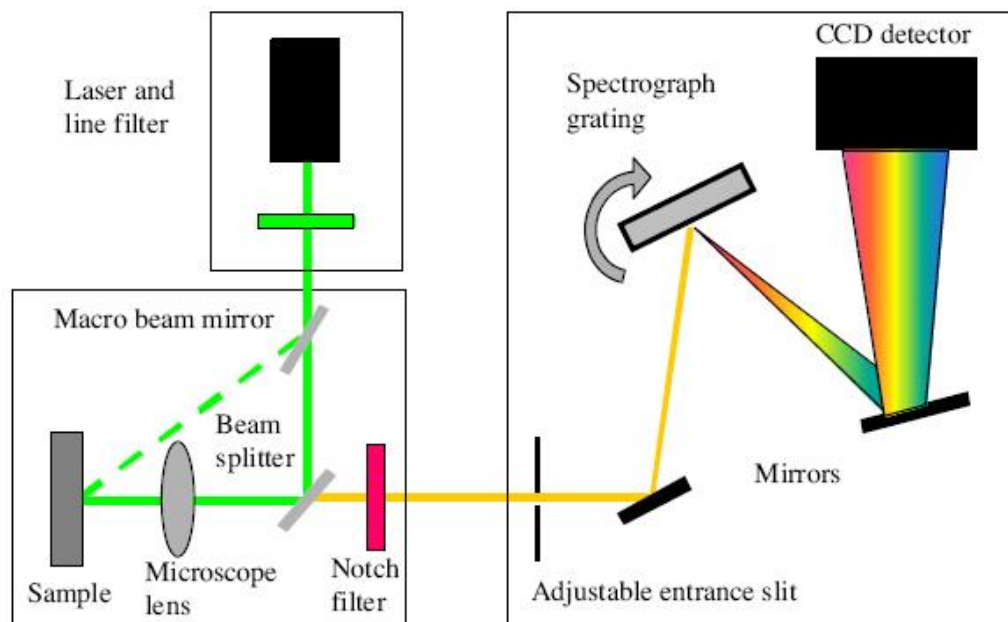


Fig. 1. A typical point Raman spectroscopy setup.

Since each molecule has a different Raman shift, one laser wavelength may be used for a large variety of species. Table 1 contains information about the characteristic Raman shifts of selected gaseous, solid and liquid species. Night time measurements are best made using lasers operating around 300-350 (3).

Molecule name	Type of substance	Raman shift (cm^{-1})
N_2	gas	2331
H_2O	gas	3460
O_2	gas	1566
H_2	gas	4155
O_2	liquid	1552

N ₂	liquid	2326.5
Benzene	liquid	992
CS ₂	liquid	655.6
Toluene	liquid	1003
SiO ₂	solid	467
LiNbO ₃	solid/crystal	256 258 637 643
LiTaO ₃	solid/crystal	201 215

Table (1) Characteristic Raman shifts of selected gaseous, solid and liquid species.

Physical Basis of the Raman Technique

Similar in approach to any optical method, Raman spectroscopy takes place through bombardment of a surface with radiation while concomitantly observing the photonic energy reaching a detector. In Raman spectroscopy, the energy that reaches the detector will be “changed” through scattering with the sample volume. The nature of this scattering, and hence the degree to which the radiation is “changed,” depends upon the distribution of phonons and electrons within the material lattice. These distributions, in turn, are both temperature and stress dependent making the interactions. Hence, the resulting Raman scattered radiation depends upon these parameters as well. Thus, the key to examine the temperature or stress dependence of the Raman scattered radiation is to understand the interaction between the incident radiation and the material lattice. Upon impingement of incident radiation to a surface, a photon with energy ε_i may be reflected, absorbed, or transmitted. In Raman spectroscopy, the concern rests solely upon an interaction in which this photon is absorbed by either an electron or, in a dramatically more unlikely case, a phonon. As part of this event, the absorbing species (i.e., the electron or phonon) is promoted from its equilibrium state of energy, ε_g , to an excited virtual state of energy, ε_L , resulting in a non-equilibrium distribution of the excited entity (see Figure 2). Simultaneously, thermalization will occur whereby this excited entity will “relax” back to its equilibrium state and distribution. Most often, this occurs directly thereby inducing the “re-emission” of a photon of energy equal to that which was incident ($\varepsilon_L - \varepsilon_g = \varepsilon_i$) in a process known as Rayleigh scattering. In a small statistical subset of these occurrences, however, an intermediate event takes place by which the excited species either absorbs or emits an additional energy carrier (i.e., phonon or electron) in the process of thermalizing as is shown in Figure 2. As a consequence of this intermediate event, the excited species moves to a secondary non-equilibrium virtual state of energy ε_m which is equal neither to its original ground (ε_g) nor excited level (ε_L). Upon relaxation of the excited entity from energy ε_m to its original equilibrium energy ε_g , a “new” photon of energy $\varepsilon_m - \varepsilon_g = \varepsilon_f$ will be emitted. Due to the

intermediate reaction, the emitted photon will have an energy unequal to that of the incident radiation ($\epsilon_f \neq \epsilon_i$) leading to what is known as inelastic scattering and Raman effect.

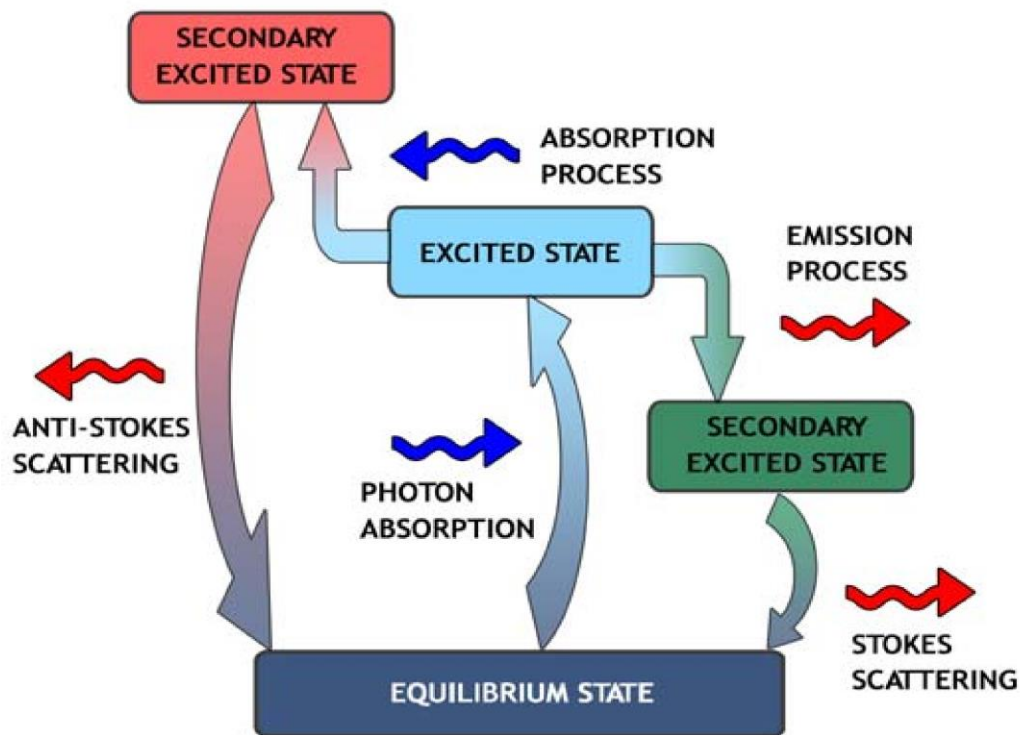


Figure (2) Change in state due to the excitation in Raman spectroscopy.

Raman spectrum

A representative figure of the resulting Raman spectrum illustrating each of these differing scattering components is shown in Figure (3). Although without notch filter the Intensity of Rayleigh events far outweighs those of the Stokes and anti-Stokes variety, its response is mitigated through the use of filters in order to highlight the specific Raman contributions.

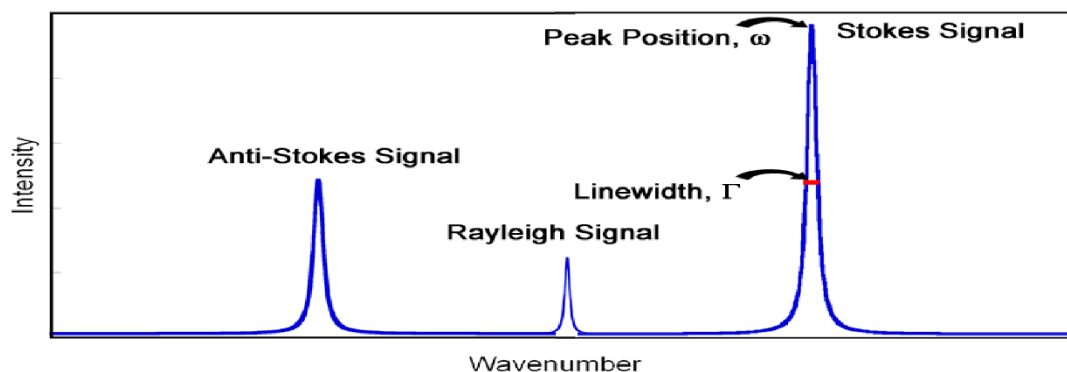


Figure (3) Representative Raman spectrum showing the Rayleigh, Stokes, and anti-Stokes responses.

Solar laser system Simulation model design:

In order to test the ability of developing a solar laser system in Helwan which is 35 km south of Cairo, the capital city of Egypt, a simulation model was developed for building such a system. A parabolic mirror was fixed in a position to track the sun as shown in Fig (4). The concentrated solar radiation is focused on a secondary compound parabolic concentrator, which is shown in Fig (5), as shown in Fig (6).

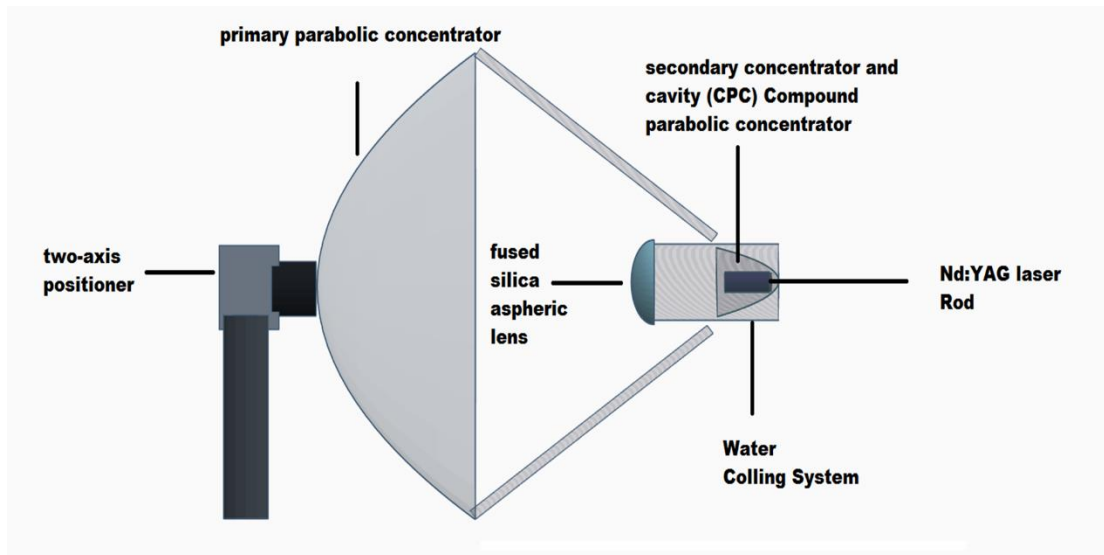


Fig. (4) Setup of the solar laser system.

CPC secondary parabolic compound reflector

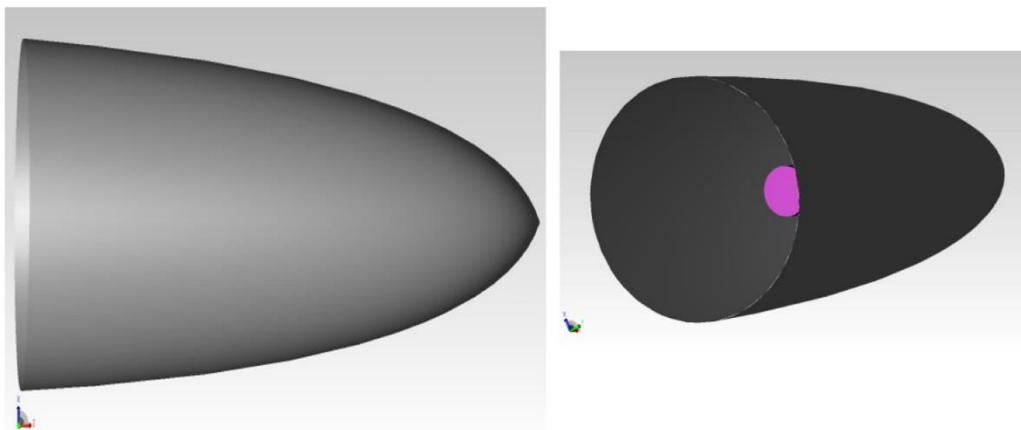


Fig. (5) The 3D Compound Parabolic Concentrator (3D-CPC).

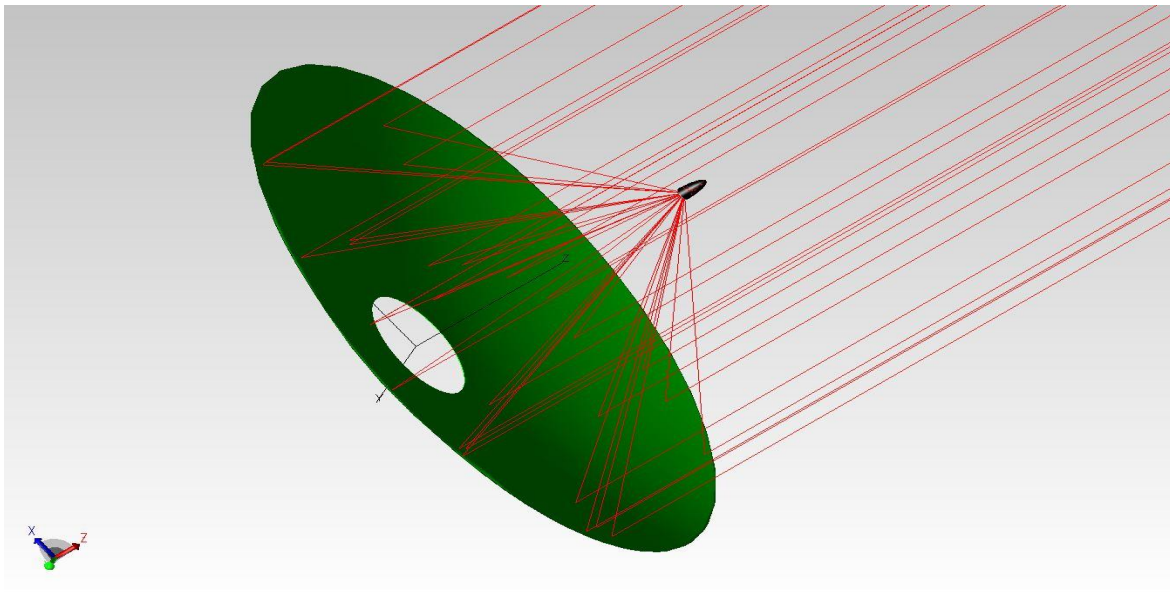


Fig (6) Solar pumped laser model scenario representation.

This concentration system will direct the radiation onto the Nd:YAG laser crystal. The laser crystal has a total reflective coating from the side of contact, while there is a partially reflective mirror at the wavelength 1064 nm as an output coupler aligned to the system on the optical bench. A water-based cooling circulation is connected to the crystal in order to eliminate the heat caused by the concentration and the laser pumping process. The whole optical system is set on a mount with a tracking motor which can let the system follow the position of the sun during the day. The parameters of the compound parabolic concentrator (CPC) are given in Table (2).

Parameter	Symbol	Value
Acceptance Angle	θ_a	20°
Concentration Ratio	C	1.483
Reflectivity	r	0.7
Height	H	30 mm

Table (2) The parameters of the 3D Compound Parabolic Concentrator (3D-CPC).

The Nd:YAG laser is the most commonly used type of solid-state laser. Neodymium-doped yttrium aluminum garnet (Nd:YAG) possesses a combination of properties uniquely favorable for laser operation.

The YAG host has a good optical quality and a high thermal conductivity. Furthermore, the cubic crystal structure of YAG produces a narrow-fluorescent line width, which results in high gain and low threshold for laser operation. In Nd: YAG, trivalent neodymium substitutes for trivalent yttrium in the lattice, so charge compensation is not required (Koechner, 1992). The parameters of the Nd: YAG laser crystal are given in Table (3).

Parameters of the used Nd:YAG laser crystal.		
Parameter	Symbol	Value
Fluorescence of the crystal	I_s	$12.5 \times 10^6 \text{ W/m}^2$
Quantum efficiency	η_q	0.63
Overlap ratio	η_{ovp}	0.14
Absorption coefficient	α	0.59
Pumping efficiency	ε	0.67
Rod length	l	0.15 mm
Rod diameter	d	3 mm

Table (3) The parameters of the Nd: YAG laser crystal.

By Using the software (Raytrace pro ©), we could calculate and estimate the distribution of the concentrated solar radiation on the laser rod. Figs. (7) and (8) show the light distribution on the side of the Nd: YAG crystal with a homogenous distribution of 60% of the total incident radiation on the primary collector in two- and three-dimensions respectively. Similarly, Figs. (9) and (10) show the distribution on the end of the Nd: YAG crystal with a homogenous distribution of 21% of the total incident radiation on the primary collector in both types of pumping direction respectively.

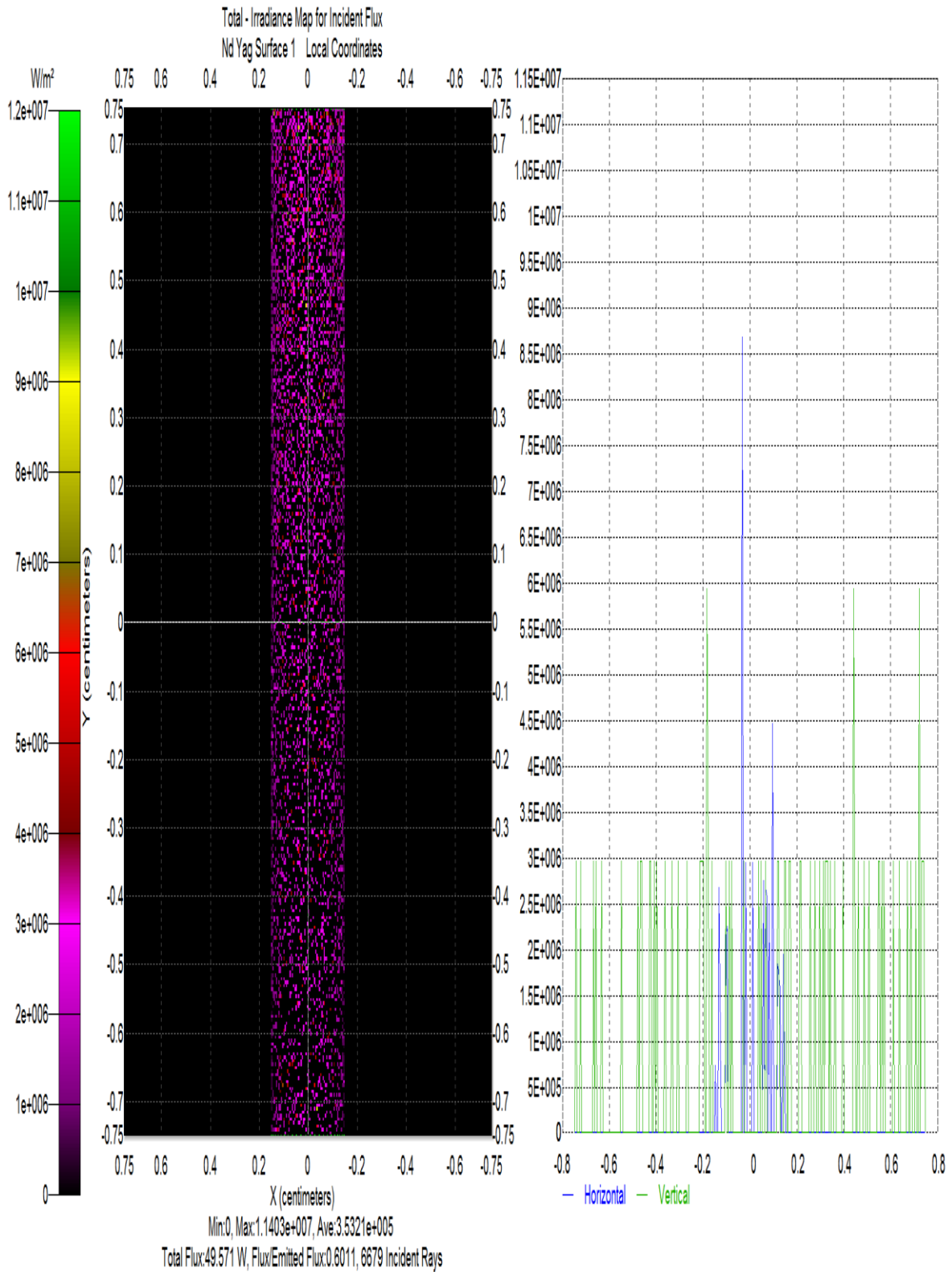
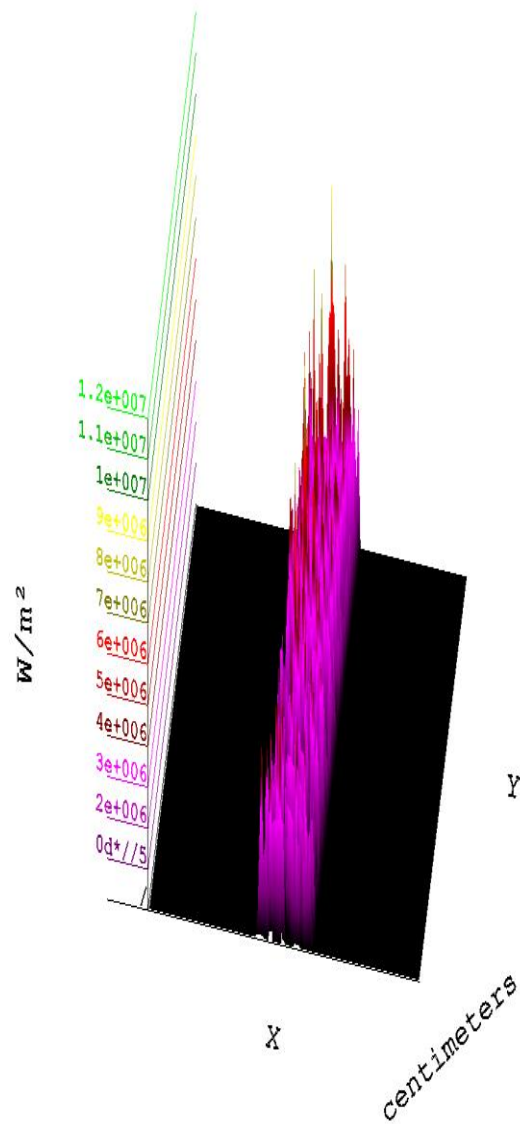


Fig (7) Two-dimensional distribution of the concentrated solar radiation on the sides of the laser rod.

Total - Irradiance Map for Incident Flux
Nd Yag Surface 1 Local Coordinates



Min:0, Max:1.1403e+007, Ave:3.5321e+005
Total Flux:49.571 W, Flux/Emitted Flux:0.6011, 6679 Incident Rays

Fig (8) Three-dimensional distribution of the concentrated solar radiation on sides of the laser rod.

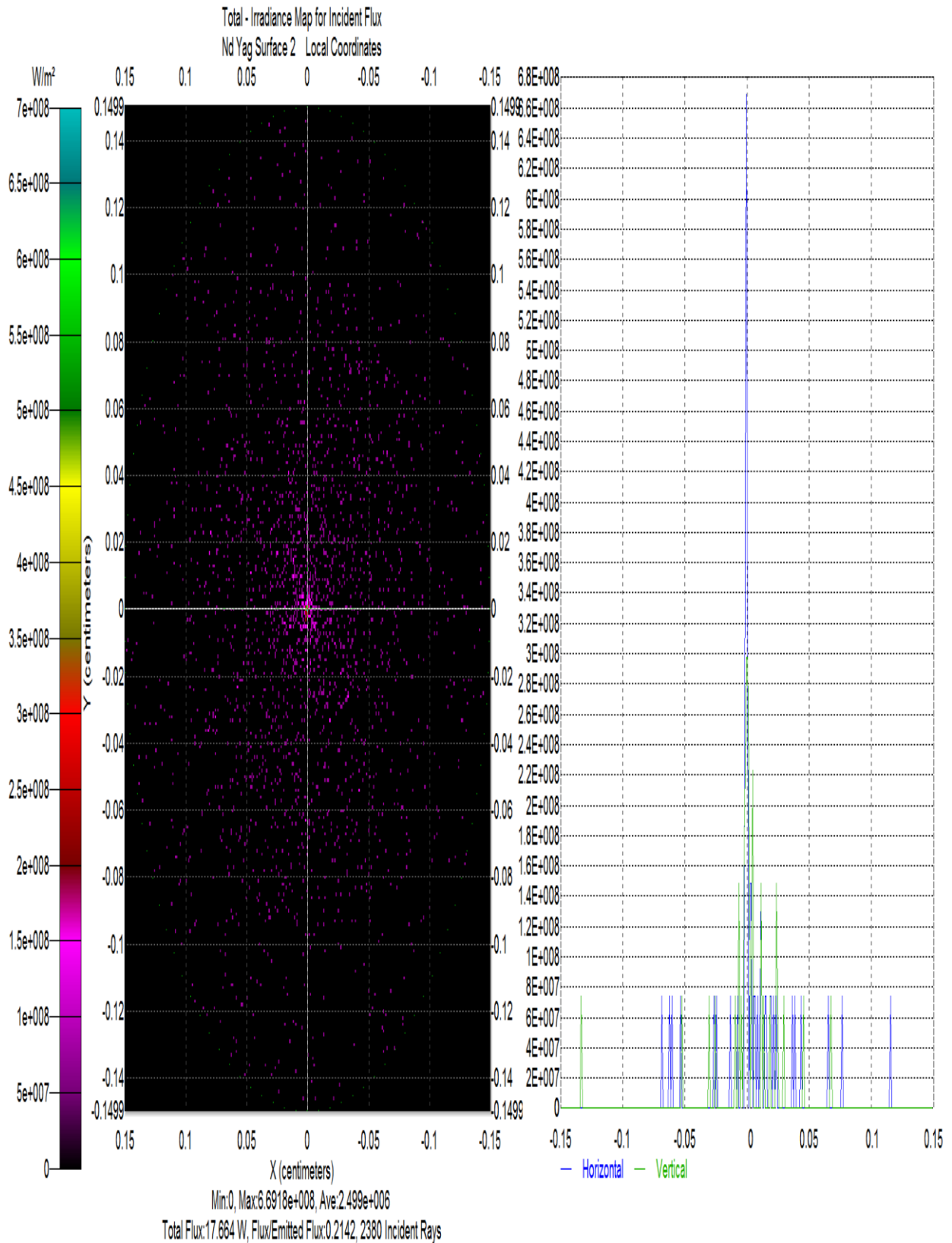
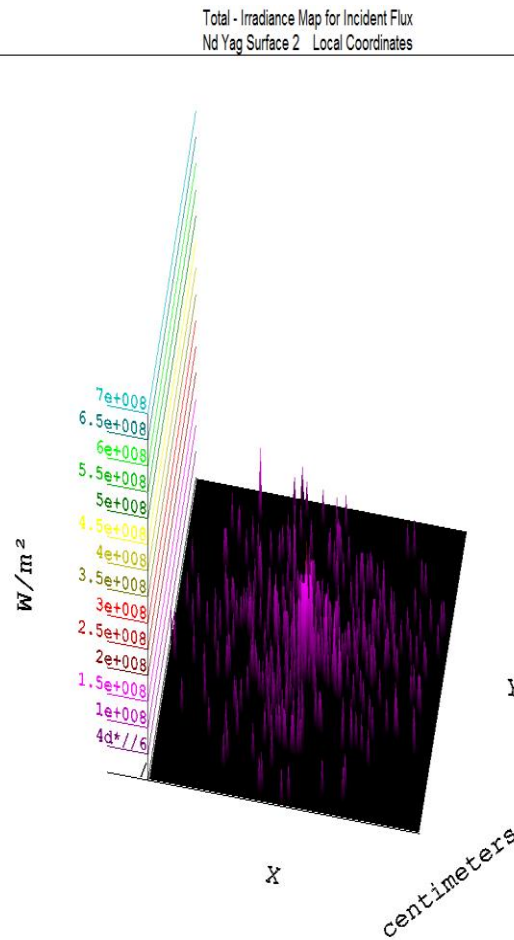


Fig. (9) Two-dimensional distribution of the concentrated solar radiation on the end of the laser rod.



Min:0, Max:6.6918e+008, Ave:2.499e+006
Total Flux:17.664 W, Flux/Emitted Flux:0.2142, 2380 Incident Rays

Fig (10) Three-dimensional distribution of the concentrated solar radiation on the end of the laser rod.

Table (4) shows the parameters of the laser rod used in this model.

#	Parameter	Value
1	Cavity length, cm	8
2	Reflectivity of output coupler	0.950
3	Active element dissipative losses, cm ⁻¹	0.015

Table (4) The laser parameters used in the model.

Laser system output

The results of our solar laser model can be summered in Table (5).

#	Parameter	Value
	In winter Average incident global radiation 320 W/m ²	
1	Full output energy, W	4.7 W
2	Full efficiency	13%
	In summer Average incident global radiation 509 w/m ²	
1	Full output energy, W	7.8 W
2	Full efficiency	13.5%
	In autumn Average incident global radiation 509 w/m ²	
1	Full output energy, W	5.9 W
2	Full efficiency	13.1%
	In spring Average incident global radiation 474 W/m ²	
1	Full output energy, W	7.268 W
2	Full efficiency	13.5%

Our Slope efficiency is 6.7%

Experimental setup for Raman spectroscopy

Fig. (11) shows the setup of using the solar laser system in Raman spectroscopy. The laser beam emitted from the system get polarized by a polarizer then focused by a lens to be directed to the sample then the Raman spectrum collected by 2 lens and a notch filter then directed to the spectrometer through a fiber optical cable.

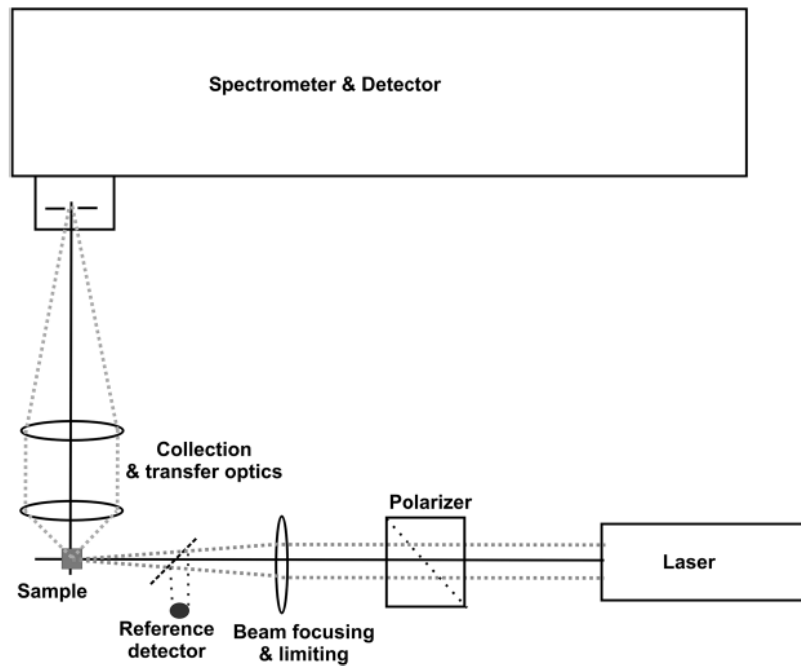


Fig. (11) Raman spectroscopy system setup.

Data acquisition

The laser light interacts with molecular vibrations, phonons or other excitons in the system resulting in the energy of the laser photons being shifted up or down. The shift in energy gives information about the vibrational modes in the system of Raman scattering of light by molecules may be used to provide information on a sample's chemical composition and molecular structure. Raman spectroscopy studies vibrational, rotational and low-frequency modes in a system.

The quantitative analysis of unknown mineral sample involves hardware equipment which is needed to perform the spectroscopy.

The individual hardware components involved in the acquisition of a spectrum is shown and it is summed up in the following steps:

1. A laser provides a (nearly) monochromatic light beam.
2. In the Raman cell laser light scatters off the sample molecules
3. The scattered light is collected by a combination of optical lenses and directed into a fiber optical tube
4. The collected light is transported by the fiber optical tube into the filter unit.
5. The notch filter is used for suppression of inelastic (elastic) Rayleigh-scattering and from diffusely reflected excitation-source light by more than six orders of magnitude.
6. In the spectrometer a grating is used for wavelength dependent diffraction.

7. The spectrum is finally detected by a CCD array detector producing a raw, two-dimensional spectrum.

Then, a software “Spectragryph © version 1.2” is used for processing the raw data

Laser Excitation Source: The used laser source is diode-pumped Neodymium-doped yttrium orthovanadate. (Nd: YVO₄/KTP) which has the wavelengths: 808 nm, 1064 nm and 532 nm. to simulate our solar laser

Raman cell: The cell design is a cage of stainless steel.

Collection Optics: The light collection optics consists of a pair of planoconvex lenses. One of them is of a focal point lies within the scattering region in the cell and the other is of a focal point that lies at the entrance of the optical fiber.

Light transport: The light is collected by an optical fiber from one of its side. The other side of the fiber is connected to the input coupling of the filter/spectrometer unit by which the fiber slit is imaged onto the CCD detector.

Filter (Rayleigh Line Suppression Filter): The spectrum which is generated inside the Raman cell does not originate from Raman scattering only. Additionally, Rayleigh scattering and inner cell reflections are collected by the fiber optics. This spectrum has the same wavelength as the excitation laser. The intensity of the Rayleigh peak alone is already at least three orders of magnitude higher than the Raman intensity [5]. In case that spectrum enters the spectrometer, the resulting stray-light would induce a spectral background which would reduce quantitative Raman measurements. For this reason, a notch filter is installed in front of the spectrometer entrance in order to suppress the light at the excitation line by more than six orders of magnitude.

CCD Camera (Spectrometer): The Stellar Net GREEN-Wave spectrometers can measure in 350-1150 nm wavelength range with an optical resolution of 0.2 nm and Detector type of CCD -2048 pixels with a high speed 16-bit digitizer allows for fast data acquisition and a signal to noise of 400:1.

Software used for spectroscopy: Spectragryph © version 1.2.

Library: RRUFF Raman mineral spectra provided by RRUFF database at University of Arizona and it was retrieved on 2017-06-12 from

http://rruff.info/zipped_data_files/raman/

Data Processing

1- Cosmic Ray Removal:

In long-term spectra recorded by CCDs, cosmic rays' events are encountered on a frequent but random basis. They (mostly) are single-pixel spikes with a much higher intensity recorded by the involved pixel in comparison to its neighbors. These cosmic ray events need to be removed prior to data analysis.

2- Removal of Low-Gain or Dead Pixel

Occasionally, CCD detectors may exhibit one or more pixels whose response differs significantly from the average over all pixels, or pixels that do not respond at all (so-called “dead” pixels). The presence of such pixels leads to singular (generally downward) spikes in the spectra. Therefore, before averaging and data analysis such events should be removed.

3- Background Removal

The task of the background removal is to discriminate the signal from the background while both are subjected to noise.

4- Analysis of Peak Intensities

The last step in the data-processing chain is the extraction of peak intensities, to be compared with the database through automated data base search

Spectral Database Search Report

Best hit: [Arrojadite NaFe \(67.27%\)](#)

spectrum info				search & results		descriptor
sample ID	ref. ID	name	method	search name	rating	Laser WL
Desktop	--	Part of: Part of:	Raman	Search_all	67.3	
	ArrojaditeNaFe	ArrojaditeNaFe__R	Raman		67.27	
	Phosphohedyp	Phosphohedyphan	Raman		63.73	
	ArrojaditeNaFe	ArrojaditeNaFe__R	Raman		62.51	
	ArrojaditeKFe	ArrojaditeKFe__R0	Raman		62.06	
	Burbankite	Burbankite__R0506	Raman		61.45	

Conclusion

A detailed Raman study on unknown mineral has been carried out. The best results obtained is Arrojadite NaFe (67.27%), which is less accurate than the ideal case due to the following

- 1- Due to the use of non-high-grade notch filter.
- 2- The use of the wavelength 532 nm, which has a low wavelength, high probability of luminescence and Rayleigh scattering.
- 3- The interference of the 808 nm, 1064 nm with the Raman signal corresponding to 532 nm due to the design of (Nd: YVO4/KTP) laser system.

Our future plans include adding other laser source to the system for more accuracy especially our 1064 nm Nd: YAG solar pumped laser. With increasing wavelength, the probability of luminescence decreases and the Rayleigh scattering does as well.

And by using the solar pumped laser system we will eliminate the interference of the diode pumping laser source and the need for 808 notch filter which will reduce the cost of the design and increase the accuracy of the system

A Super Notch filter will be added to the system to increase its accuracy with the following Parameters:

- Standard wavelengths: 532,785, 1064 nm.
- Coefficient of suppression of laser radiation $>10^6$.
- Transmission outside the notch from 460 nm to 1500nm, 90%.
- Spectral bandwidth of a notch: < 25 nm.

References

- [1] Weksler MS 1988 Solar-pumped solid-state lasers, *IEEE J. Quantum Electron.* **24** 1222–1228.
- [2] Krupkin V 2016 , Non imaging optics and solar laser pumping at the Weizmann Institute ,*Proc . SPIE* (1993) **50–60**.
- [3] Abdel-Hadi YA, 2006. Development of Optical Concentrator Systems for Directly Solar Pumped Laser Systems. *Mensch und Buch Verlag*, Berlin, Germany
- [4] Koechner W 1992. Solid-state laser engineering, third ed. In: *Springer Series in Optical Science*, vol. **1** Springer Verlag.
- [5] Sharma S K. (2005) "Portable remote Raman system for monitoring hydrocarbon, gas hydrates and explosives in the environment", *Spechtrichimica Acta* Part A **61**, 2404 – 2412
- [6] Menzel E R. 1995. *Laser Spectroscopy: Techniques and Applications*, Marcel Dekker, New York
- [7] Dzianis P 2007 Computer simulation of stand-off LIBS and Raman LIDAR for remote sensing of distant compounds,
- [8] Beechem T E. 2008 METROLOGY OF GaN ELECTRONICS USING MICRO-RAMAN SPECTROSCOPY A Thesis Presented to The Academic Faculty By III In Partial Fulfillment Of the Requirements for the Degree Doctor of Philosophy in Mechanical Engineering Georgia Institute of Technology
- [9] Schlösser M, Springer Theses Recognizing Outstanding Ph.D. Research Accurate Calibration of Raman Systems At the Karlsruhe Tritium Neutrino Experiment
- [10] Neumann (2015) *Wilfried (Press Monograph)* Applications of dispersive optical spectroscopy systems- Society of Photo Optical SPIE Press